


Open Access Article

 <https://doi.org/10.55463/issn.1674-2974.50.6.9>

The Resonance of Septic Nonlinearity of the Forced and Damped Duffing Oscillator

Lubna Naz Arain¹, Imran Qasim Memon², Asghar Ali Maitlo³, Muhammad Afzal Soomro³,
Sanaullah Dehraj^{3*}, Rajab Ali Malookani³, Asif Mehmood Awan⁴

¹ Department of Natural Sciences, Begum Nusrat Bhutto Women University, Sukkur, Sindh, Pakistan

² Department of Basic Science and Related Studies, Mehran University of Engineering and Technology, Jamshoro, Sindh, Pakistan

³ Department of Mathematics and Statistics, Quaid-e-Awam University of Engineering, Science and Technology, 67480 Nawabshah, Sindh, Pakistan

⁴ Department of Artificial Intelligence and Mathematical Sciences, Sindh Madressatul Islam University, Karachi, Pakistan

* Corresponding author: sanaullahdehraj@quest.edu.pk

Received: March 16, 2023 / Revised: April 10, 2023 / Accepted: May 7, 2023 / Published: June 30, 2023

Abstract: The aim of this paper is to study the dynamics of a nonlinear damped Duffing oscillator under the influence of weak and strong harmonically time-varying external excitation. The mathematical Duffing oscillator is represented by a nonhomogeneous second-order ordinary differential equation with a seventh degree of nonlinearity. The approximate analytical solution of the governing equation is obtained in terms of amplitude and frequency responses via the application of a two timescale perturbation method. The two timescale perturbation method is used to find (un)steady state solution of the Duffing oscillator for weakly and strongly external harmonic excitation. It is found that the amplitude response decays as time increases due to the presence of damping in the system. In addition, the forcing and septic nonlinearity parameters are found to be dominated by the nonlinearity and amplitude of the system.

Keywords: damped duffing oscillator, external excitation, two timescale perturbation method, resonance.

受迫阻尼达芬振荡器的脓毒非线性共振

摘要： 本文的目的是研究弱谐波时变外部激励和强谐波时变外部激励影响下非线性阻尼达芬振荡器的动力学。数学达芬振子由具有七阶非线性的非齐次二阶常微分方程表示。通过应用两时间尺度扰动方法，根据振幅和频率响应获得了控制方程的近似解析解。两时间尺度扰动方法用于寻找弱和强外部谐波激励的达芬振荡器的(非)稳态解。研究发现，由于系统中存在阻尼，振幅响应随着时间的增加而衰减。此外，发现强迫和败坏非线性参数受系统的非线性和振幅支配。

关键词： 信息管理模型，短期规划，年度运营计划，伊达尔戈理工大学。

Introduction

The nonlinear Duffing oscillator has a wide range of applications in science, engineering, biology, and communication theory, including soliton theory, for example, magnetoelastic mechanical structures, huge amplitude oscillation of centrifugal governor structures, nonlinear vibration of beams and plates, and fluid flow persuaded vibration. Few issues occurring in different fields of applied sciences and engineering are linear whereas many oscillation problems are nonlinear. Nonlinear oscillations are important in physical sciences, mechanical structures, and other disciplines, which are mathematically expressed in the form of differential equations; most of them are nonlinear. The methods of solving linear differential equations are comparatively easy and well established. On the contrary, the solution techniques of nonlinear differential equations are less available, and in general, linear approximations are frequently used. It is very difficult to solve nonlinear differential equations, and in general, it is often more difficult to obtain an analytic approximation than a numerical one. To overcome this shortcoming, in recent years, many analytical and numerical methods have been used for solving these nonlinear differential equations. For instance, Lindstedt-Poincare perturbation method [1-4], multiple scale perturbation method [5-15], Homotopy perturbation method [16-17], energy balance method [18-19], modified variational approach [20-22], Adomian decomposition method [23-27], and Laplace transform method [28-29]. The amplitude–frequency relationship is important for the accurate prediction of nonlinear oscillatory systems in many areas of physics and engineering, especially in nonlinear structural dynamics. Therefore, the analysis of nonlinear systems has been widely considered. In recent years, many powerful methods have been used to find approximate solutions and the amplitude-frequency relationship to nonlinear differential equations. The two timescale perturbation method is one of the most suitable methods to investigate the nonlinear dynamics of oscillators. In the literature, the dynamic behavior of the Duffing oscillator up to degree five is studied. However, it is still very interesting to examine the behavior of the forced Duffing oscillator up to degree seven of nonlinear terms. This study finds (un)steady-state responses for (non)resonance phenomena for a forced Duffing oscillator with septic nonlinearity. The following governing equations of motion [30] for the Duffing oscillator under septic nonlinearity with initial conditions are given as follows:

$$\frac{d^2u}{dt^2} + \delta \frac{du}{dt} + \alpha u + \beta u^3 + \gamma u^5 + \mu u^7 = F(t) \quad (1)$$

$$u(0) = x_0, \quad \frac{du}{dt}(0) = x_1 \quad (2)$$

where $\alpha > 0$, $\beta > 0$, $\gamma > 0$, $\mu > 0$ represents hard spring, $\alpha < 0$, $\beta < 0$, $\gamma < 0$, $\mu < 0$ represents

softening spring, $F(t)$ represents external harmonic excitation. The damping coefficients are represented by δ and x_0 , x_1 represent the initial displacement and initial velocity, respectively. In Eq. (1), α is taken as ω^2 as a natural frequency of the Duffing oscillator and the external excitation as a harmonically excited system, that is $F(t) = F_0 \cos(\Omega t)$, where F_0 is the amplitude of external excitation and Ω as the excitation frequency. In this paper, Eq. (1) has been studied for two different cases of external excitations, i.e. $F(t) = O(\epsilon)$ and $F(t) = O(1)$. In the next section, the initial-value problem for two different cases of external excitations will be studied via a two timescale perturbation method.

1. Weakly Excited System $F(t) = O(\epsilon)$

Let us consider that the external excitation $F(t)$, damping δ and nonlinear coefficients β , γ and μ are considered to be of $O(\epsilon)$. Based upon these assumptions, Equations (1) and (2) become as follows:

$$\frac{d^2u}{dt^2} + \omega^2 u + \epsilon \left[\delta \frac{du}{dt} + \beta u^3 + \gamma u^5 + \mu u^7 \right] = \epsilon F_0 \cos(\Omega t) \quad (3)$$

$$u(0) = x_0, \quad \frac{du}{dt}(0) = x_1 \quad (4)$$

1.1. Application of a Two Timescale Perturbation Method

This subsection will study the governing equations of motion given in Equations (3) and (4) by the application of a two timescale perturbation method. Let us consider that the solution of Eq. (3) is of the form given as:

$$u(t) = u(T_0, T_1; \epsilon) \quad (5)$$

where the time T_0 is a fast scale and T_1 is a slow scale, that is: $T_0 = t$ and $T_1 = \epsilon t$. The transformation of derivatives with these fast T_0 and slow timescales T_1 then becomes:

$$\begin{aligned} \frac{d}{dt} &= \frac{\partial}{\partial T_0} + \epsilon \frac{\partial}{\partial T_1} + \dots \\ \frac{d^2}{dt^2} &= \frac{\partial^2}{\partial T_0^2} + 2\epsilon \frac{\partial^2}{\partial T_0 \partial T_1} + \dots \end{aligned} \quad (6)$$

By setting Equations (5) and (6) into Eq. (3) it yields:

$$\begin{aligned} \left[\frac{\partial^2 u}{\partial T_0^2} + 2\epsilon \frac{\partial^2 u}{\partial T_0 \partial T_1} + \dots \right] + \omega^2 u \\ + \epsilon \left[\delta \left(\frac{\partial u}{\partial T_0} + \epsilon \frac{\partial u}{\partial T_1} + \dots \right) + \beta u^3 \right. \\ \left. + \gamma u^5 + \mu u^7 \right] = \epsilon F_0 \cos(\Omega t) \end{aligned} \quad (7)$$

The expansion of Eq. (5) is in the following form:

$$\begin{aligned} u(t) &= u(T_0, T_1; \epsilon) \\ &= u_0(T_0, T_1) + \epsilon u_1(T_0, T_1) \\ &\quad + O(\epsilon^2) \end{aligned} \quad (8)$$

By putting Eq. (8) into Eq. (7) and equating the

coefficients of various powers of ϵ^0 and ϵ^1 , $O(1)$ and $O(\epsilon)$ – problem is obtained as follows:

$$O(1): \frac{\partial^2 u_0}{\partial T_0^2} + \omega^2 u_0 = 0 \quad (9)$$

$$O(\epsilon): \frac{\partial^2 u_1}{\partial T_0^2} + \omega^2 u_1 = -2 \frac{\partial^2 u_0}{\partial T_0 \partial T_1} - \delta \frac{\partial u_0}{\partial T_0} - \beta u_0^3 - \gamma u_0^5 - \mu u_0^7 + F_0 \cos(\Omega T_0) \quad (10)$$

The solution of $O(1)$ problem given in Eq. (9) can be obtained directly by integration that is given as follows:

$$u_0 = A(T_1)e^{i\omega T_0} + \bar{A}(T_1)e^{-i\omega T_0} \quad (11)$$

where the function $A(T_1)$ is defined as follows:

$$A(T_1) = \frac{1}{2} a(T_1) e^{ib(T_1)} \quad (12)$$

The functions $a(T_1)$ and $b(T_1)$ can be obtained by eliminating the secular terms from $O(\epsilon)$ the problem. By putting Eq. (11) into Eq. (10), it yields:

$$\begin{aligned} \frac{\partial^2 u_1}{\partial T_0^2} + \omega^2 u_1 = & -2 \left[\frac{\partial^2}{\partial T_0 \partial T_1} \{Ae^{i\omega T_0} + \bar{A}e^{-i\omega T_0}\} \right] \\ & - \delta \left[\frac{\partial}{\partial T_0} \{Ae^{i\omega T_0} + \bar{A}e^{-i\omega T_0}\} \right] \\ & - \beta [Ae^{i\omega T_0} + \bar{A}e^{-i\omega T_0}]^3 \\ & - \gamma [Ae^{i\omega T_0} + \bar{A}e^{-i\omega T_0}]^5 \\ & - \mu [Ae^{i\omega T_0} + \bar{A}e^{-i\omega T_0}]^7 \\ & + F_0 \cos(\Omega T_0) \end{aligned} \quad (13)$$

After lengthy calculations, it turns out that the resonances on the right-hand side of Eq. (13) occur if the excitation frequency Ω is equal to the natural frequency ω of the system, that is, $\Omega = \omega$. This resonance is known as primary resonance.

1.2. Amplitude-Frequency Response of the System at Primary Resonance: $\Omega \cong \omega$

To show the nearness of Ω to ω , one may use detuning parameters:

$$\Omega = \omega + \epsilon\sigma \quad (14)$$

where the parameter σ is taken to be $O(1)$. By putting Eq. (14) into Eq. (13), the secular (unbounded) terms on the right hand side of Eq. (13) is obtained, which will violate the uniformity condition for the asymptotic expansion (8). To obtain uniform asymptotic approximations, the secular terms on the right-hand side of Eq. (13) will be eliminated after plugging Eq. (14). Thus, the elimination of secular term yield:

$$\begin{aligned} 2i\omega \frac{\partial A}{\partial T_1} + \delta i\omega A + 3\beta A^2 \bar{A} + 10\gamma A^3 \bar{A}^2 + 35\mu A^4 \bar{A}^3 \\ - \frac{1}{2} F_0 e^{i\sigma T_1} = 0 \end{aligned} \quad (15)$$

In order to solve Eq. (15) for the function $A(T_1)$, $A = \frac{1}{2} a e^{ib}$ will be put into Eq. (15) and separate the real and imaginary parts to get:

$$\dot{a} = -\frac{1}{2} \delta a + \frac{F_0}{2\omega} \sin(\sigma T_1 - b) \quad (16)$$

$$\begin{aligned} a\dot{b} = & \frac{3}{8\omega} \beta a^3 + \frac{10}{32\omega} \gamma a^5 + \frac{35}{128\omega} \mu a^7 \\ & - \frac{F_0}{2\omega} \cos(\sigma T_1 - b) \end{aligned} \quad (17)$$

Equations (16) and (17) are non-autonomous systems, that is, the system that depends upon the independent variable time T_1 in this case. To write them independent of time variables, it follows $\eta = \sigma T_1 - b$, so $b = \sigma T_1 - \eta$ or $b' = \sigma - \eta'$. With these substitutions, Equations. (16) and (17) becomes:

$$\dot{a} = -\frac{1}{2} \delta a + \frac{F_0}{2\omega} \sin\eta \quad (18)$$

$$\begin{aligned} a\dot{\eta} = & a\sigma - \frac{3}{8\omega} \beta a^3 - \frac{10}{32\omega} \gamma a^5 - \frac{35}{128\omega} \mu a^7 \\ & + \frac{F_0}{2\omega} \cos\eta \end{aligned} \quad (19)$$

Equations (18) and (19) can be solved for the amplitude-response a and phase η or alternatively for b . It is not easy to solve the system of ordinary differential equations given in (18)-(19) analytically, so they will be solved numerically. The numerical Runge-Kutta method is used to solve Equations (18) and (19), and the solution is shown in Fig. 1.

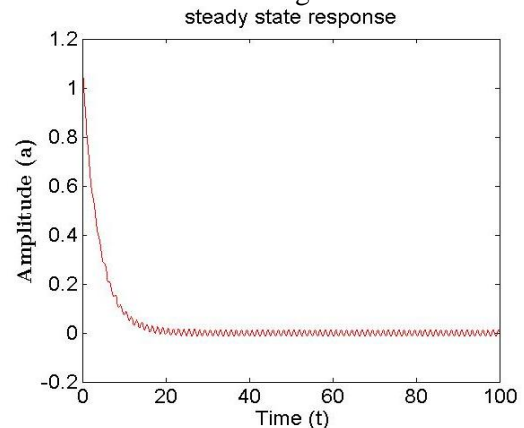


Fig. 1 Steady-state response for $\omega = 2$, $\delta = 0.5$, $\beta = 10$, $\gamma = 10$, $\mu = 100$, $F_0 = 0.4$

It can clearly be seen from Fig. 1 that the amplitude response a reduces to zero as the time t increases, so a steady-state solution is possible for a weakly excited system at the primary resonance.

1.3. Steady-State Solution in Terms of Frequency Response Curve

For steady state solution, the time-dependent term is zero into Equations (18) and (19), that is $a' = 0$, and $\eta' = 0$, it follows:

$$\dot{a} = 0 \Rightarrow \frac{\delta a}{2} = \frac{F_0}{2\omega} \sin\eta \quad (20)$$

$$\begin{aligned} \dot{\eta} = 0 \Rightarrow & a\sigma - \frac{3}{8\omega} \beta a^3 - \frac{5}{16\omega} \gamma a^5 - \frac{35}{128\omega} \mu a^7 \\ & = -\frac{1}{2\omega} F_0 \cos\eta \end{aligned} \quad (21)$$

After squaring and adding Equations (20) and (21)

and putting $\sigma = \frac{1}{\epsilon}(\Omega - \omega)$, the following expression for the frequency response curve is obtained:

$$\frac{\Omega}{\omega} = 1 + \frac{\epsilon}{\omega} \left[\frac{3}{8\omega} \beta a^2 + \frac{5}{16\omega} \gamma a^4 + \frac{35}{128\omega} \mu a^6 \right] \pm \frac{1}{2} \sqrt{\left(\frac{F^2}{a^2 \omega^2} - \delta^2 \right)} \quad (22)$$

where $\delta < \frac{F}{a\omega}$.

Fig. 2 depicts that there is a reasonable effect of septic nonlinearity on the amplitude and frequency. It is shown that the amplitude a bends to the right for positive values of the septic nonlinear parameter μ (Fig. 2a), while for negative values of the parameter, the amplitude a bends to the left (Fig. 2b). However, the effect of septic nonlinearity μ is very rare when the values of damping parameters reduce δ .

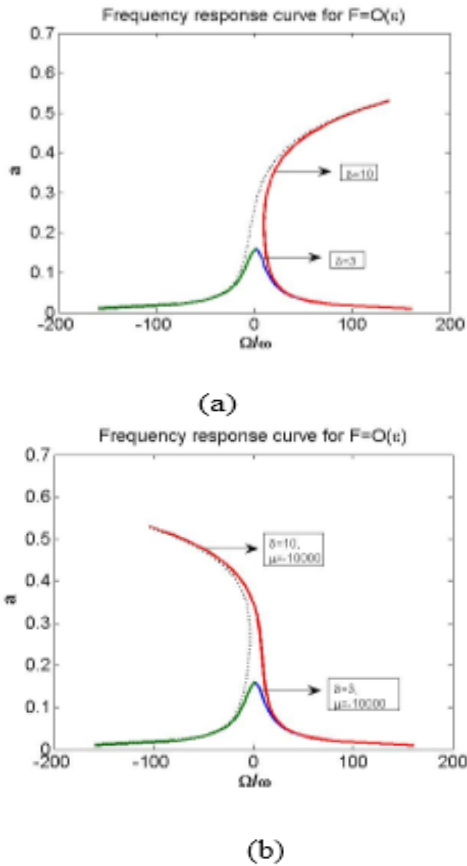


Fig. 2 Variation of amplitude with frequency (a) $\delta > 0$ (b) $\delta, \mu < 0$ $\omega = 2$, $\beta = 10$, $\gamma = 10$, $R = 0.1$

The effects of septic nonlinearity and the amplitude of excitation on the amplitude a and the frequency ratio $\frac{\Omega}{\omega}$ are shown in Fig. 3. It can be clearly seen in Fig. 3a where the amplitude a shifts to the left as the positive nonlinear parameter μ reduces, while the frequency ratio $\frac{\Omega}{\omega}$ versus amplitude a converges to zero if the values of amplitude of excitation decrease.

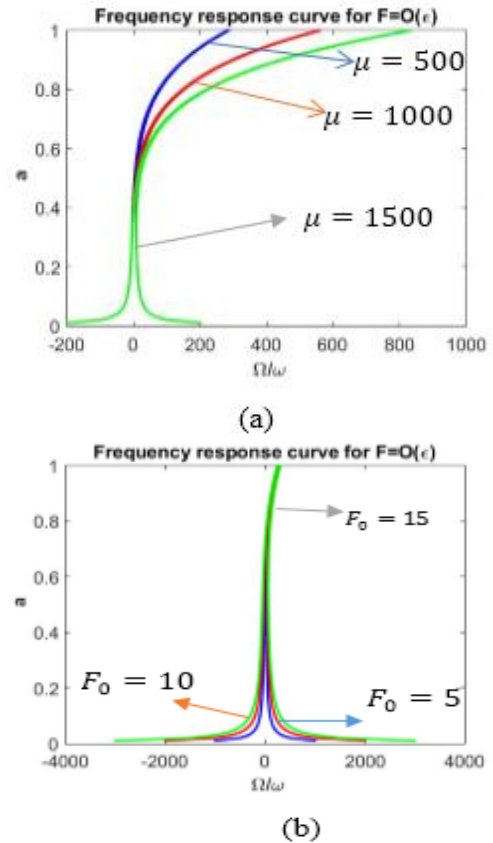


Fig. 3 Variation of amplitude with frequency (a) under septic nonlinearity and (b) forcing term for $\omega = 2$

2. Strongly Excited System $F(t) = O(1)$

This section will study the damped Duffing oscillator under the effect of external excitation of $O(1)$, that is, $F(t) = O(1)$ and damping parameter δ and nonlinear parameter β, γ and μ are considered to be of $\delta = O(\epsilon)$, $\beta = O(\epsilon)$, $\gamma = O(\epsilon)$, $\mu = O(\epsilon)$. Based upon these assumptions the governing Eq. (1) becomes as follow:

$$\frac{d^2 u}{dt^2} + \omega^2 u + \epsilon \left[\delta \frac{du}{dt} + \beta u^3 + \gamma u^5 + \mu u^7 \right] = F_0 \cos(\Omega t) \quad (23)$$

In the next subsection, Eq. (23) will be studied via a two timescale perturbation method.

2.1. Application of a Two Timescale Perturbation Method

To construct the approximate analytical solution of Eq. (23), a two timescale perturbation method will be used. By using Equations (5), (6), and (8) and by collecting the terms of $O(1)$ and $O(\epsilon)$ following problems are obtained:

$$O(1): \frac{\partial^2 u_0}{\partial T_0^2} + \omega^2 u_0 = F_0 \cos(\Omega T_0) \quad (24)$$

$$O(\epsilon): \frac{\partial^2 u_1}{\partial T_0^2} + \omega^2 u_1 = -2 \frac{\partial^2 u_0}{\partial T_0 \partial T_1} - \delta \frac{\partial u_0}{\partial T_0} - \beta u_0^3 - \gamma u_0^5 - \mu u_0^7 \quad (25)$$

Eq. (24) is a nonhomogeneous linear differential equation with variable coefficients. The general solution of Eq. (24) is obtained as:

$$u_0 = A(T_1)e^{i\omega T_0} + Re^{i\Omega T_0} + cc \quad (26)$$

where $A = \frac{1}{2}ae^{ib}$, and $R = \frac{F_0}{2(\omega^2 - \Omega^2)}$, and where cc denotes the complex conjugate. The functions a and b are the functions of slow timescale T_1 and can be determined by eliminating the secular terms from the $O(\epsilon)$ problem. Putting Eq. (26) into Eq. (25), it follows:

$$\begin{aligned} & \frac{\partial^2 u_1}{\partial T_0^2} + \omega^2 u_1 \\ &= -2 \frac{\partial^2}{\partial T_0 \partial T_1} [A(T_1)e^{i\omega T_0} + Re^{i\Omega T_0} + cc] \\ & - \delta \frac{\partial}{\partial T_0} [A(T_1)e^{i\omega T_0} + Re^{i\Omega T_0} + cc] \\ & - \beta [A(T_1)e^{i\omega T_0} + Re^{i\Omega T_0} + \bar{A}(T_1)e^{i\omega T_0} + Re^{-i\Omega T_0}]^3 \\ & - \gamma [A(T_1)e^{i\omega T_0} + Re^{i\Omega T_0} + \bar{A}(T_1)e^{i\omega T_0} + Re^{-i\Omega T_0}]^5 \\ & - \mu [A(T_1)e^{i\omega T_0} + Re^{i\Omega T_0} + \bar{A}(T_1)e^{i\omega T_0} \\ & + Re^{-i\Omega T_0}]^7 \end{aligned} \quad (27)$$

On the right hand side of Eq. (27), resonances occur if the excitation frequency Ω is equal to the natural frequency ω of the system, that is, resonances occur if:

- $\Omega = \omega, 3\omega, 5\omega, 7\omega$ (subharmonic Resonances),
- $\Omega = \frac{1}{3}\omega, \frac{1}{5}\omega, \frac{1}{7}\omega$ (super-harmonic resonance).

2.2. Non-Resonant Case

In this case, the excitation frequency Ω is taken away from the natural frequency ω of the system, that is, $\Omega \neq \omega, 2\omega, 3\omega, 5\omega, 7\omega, \frac{1}{2}\omega, \frac{1}{3}\omega, \frac{1}{5}\omega, \frac{1}{7}\omega$. In this situation, the elimination of secular terms on the right hand side of Eq. (27) yields:

$$\begin{aligned} & 2i\omega \frac{\partial A}{\partial T_1} + \delta\omega iA + \beta(3A^2\bar{A} + 6AR^2) \\ & + \gamma(10A^3\bar{A}^2 + 60R^2A^2\bar{A} \\ & + 30R^4A) \\ & + \mu(35A^4\bar{A}^3 + 420R^2A^3\bar{A}^2 \\ & + 630R^4A^2\bar{A} + 140R^6A) \\ & = 0 \end{aligned} \quad (28)$$

The solution of Eq. (28) for the function A is put $A = \frac{1}{2}ae^{ib}$ into Eq. (28) and separating the real and imaginary parts and it yields below.

2.2.1. Imaginary Part

$$\omega \dot{a} + \frac{1}{2}\delta\omega a = 0 \quad (29)$$

With $\omega \neq 0$, the solution of Eq. (29) is obtained as:

$$a(T_1) = Ke^{-\frac{1}{2}\delta T_1} \quad (30)$$

where K is an arbitrary constant and can be determined by initial conditions.

2.2.2. Real Part

$$\begin{aligned} \omega \frac{\partial b}{\partial T_1} = & 3\beta \left[R^2 + \frac{1}{8}a^2 \right] \\ & + \gamma \left[3R^4 + \frac{1}{12}a^2R^2 + \frac{1}{16}a^4 \right] \\ & + 35\mu \left[2R^6 + \frac{9}{4}a^2 + \frac{3}{8}a^4R^2 \right. \\ & \left. + \frac{1}{128}a^6 \right] \end{aligned} \quad (31)$$

Substitution of Eq. (30) into Eq. (31) yields:

$$\begin{aligned} b(T_1) = & \frac{3\beta}{\omega} \left[T_1R^2 - \frac{1}{8\delta}K^2e^{-\delta T_1} \right] \\ & + 5\frac{\gamma}{\omega} \left[3R^4T_1 - \frac{1}{12\delta}R^2K^2e^{-\delta T_1} \right. \\ & \left. - \frac{1}{32\delta}K^4e^{-2\delta T_1} \right] \\ & + 35\frac{\mu}{\omega} \left[2R^6T_1 - \frac{9}{4\delta}R^4K^2e^{-\delta T_1} \right. \\ & \left. - \frac{3}{16\delta}R^2K^4e^{-2\delta T_1} \right. \\ & \left. - \frac{1}{584\delta}K^6e^{-3\delta T_1} \right] + b_0 \end{aligned} \quad (32)$$

where b_0 is an arbitrary constant. Thus, the amplitude response of the Duffing oscillator in the non-resonant case is obtained:

$$\begin{aligned} u(t) = & \frac{1}{2}a(T_1)e^{(\omega T_0 + b(T_1))i} + \frac{F_0}{2(\omega^2 - \Omega^2)}e^{i\Omega T_0} \\ & + cc + O(\epsilon) \end{aligned} \quad (33)$$

The amplitude response of the doffing oscillator under non-resonant cases is obtained in Eq. (33) and is shown in Fig. 4. It can be clearly seen that the free oscillation solution decays as the time increases and hence the steady state response consists of forced solution only similar to the linear case.

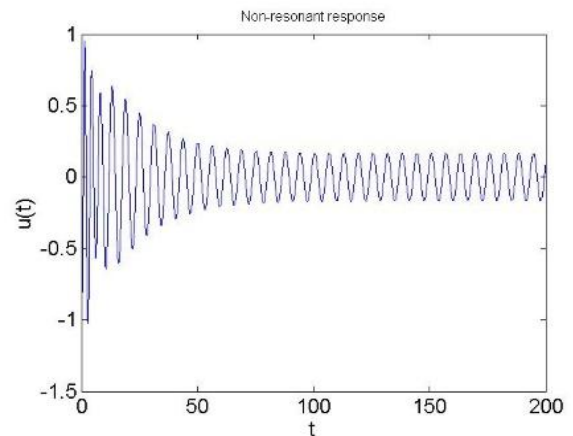


Fig. 4 Amplitude-response for $\omega = 2, \Omega = 1, \delta = 1, \beta = 10, \gamma = 10, \mu = 100, F_0 = 4$

2.3. Resonant Case

In this subsection, the amplitude response of the damped Duffing oscillator will be computed at the resonances, i.e., when the excitation frequency Ω is taken as close to the natural frequency ω of the system. This study is restricted to the following resonant cases:

$$\Omega = 5\omega, \frac{1}{5}\omega, 7\omega \text{ and } \frac{1}{7}\omega.$$

2.3.1. Case-1: When $\Omega \cong 5\omega$ (Subharmonic Resonance)

In order to show the nearness of excitation frequency Ω to the 5 times natural frequency of the system, the detuning parameter σ is introduced as $\Omega = 5\omega + \varepsilon\sigma$, where σ is taken to be $O(1)$. The substitution of $\Omega = 5\omega + \varepsilon\sigma$ into Eq. (27) and the elimination of secular terms in the resulting equation, the following two equations after separating the real and imaginary parts are obtained.

Imaginary part:

$$a' = -\frac{\delta a}{2} - \frac{1}{w} \left(\frac{5}{16} Ra^4 \gamma + \frac{35}{64} \mu Ra^6 + \frac{35}{16} \mu R^3 a^4 \right) \sin(\sigma T_1) - 5b \tag{34}$$

Real part:

$$ab' = \frac{5}{\omega} \left[\beta \left(\frac{3}{8} a^3 + 3R^2 a \right) + \frac{\gamma}{\omega} \left(\frac{5}{16} a^5 + \frac{15}{2} R^2 a^3 + 15R^4 a \right) + \frac{\mu}{\omega} \left(\frac{35}{128} a^7 + \frac{105}{8} R^2 a^5 + \frac{315}{4} R^4 a^3 + 70R^6 a \right) \right] + \frac{5}{\omega} \left(\frac{5}{16} Ra^4 \gamma + \frac{42}{64} \mu Ra^6 + \frac{35}{16} \mu R^3 a^4 \right) \cos(\sigma T_1) - 5b \tag{35}$$

Equations (34) and (35) are non-autonomous systems that depend on the time variable. To make it an autonomous system:

$$b = \frac{1}{5}(\sigma T_1 - \eta) \Rightarrow b' = \frac{1}{5}(\sigma - \eta') \tag{36}$$

By putting Eq. (36) into Equations (34) and (35) it yields:

$$a' = -\frac{\delta a}{2} - \frac{1}{w} \left(\frac{5}{16} Ra^4 \gamma + \frac{35}{64} \mu Ra^6 + \frac{35}{16} \mu R^3 a^4 \right) \sin \eta \tag{37}$$

$$a\eta' = a\sigma - \frac{5}{\omega} \left[\beta \left(\frac{3}{8} a^3 + 3R^2 a \right) + \frac{\gamma}{\omega} \left(\frac{5}{16} a^5 + \frac{15}{2} R^2 a^3 + 15R^4 a \right) + \frac{\mu}{\omega} \left(\frac{35}{128} a^7 + \frac{105}{8} R^2 a^5 + \frac{315}{4} R^4 a^3 + 70R^6 a \right) \right] \tag{38}$$

Equations (37) and (38) are not easy to solve analytically. Thus, the numerical Runge-Kutta method is used to solve them numerically. The numerical solution of the system given in Equations (37) and (38) in terms of amplitude is shown in Fig. 5. It can clearly be seen that the amplitude response a gets to zero as the time t progresses. Hence, the steady-state response is only possible for the Duffing oscillator at the subharmonic resonance, that is, at $\Omega = 5\omega$.

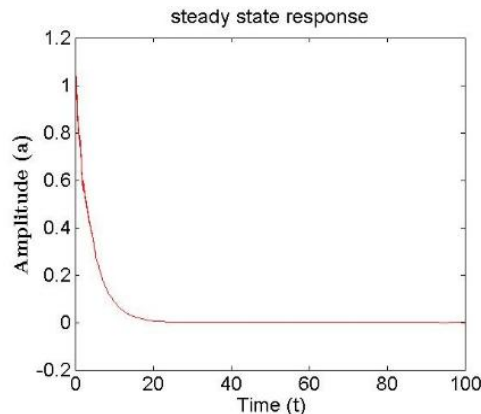


Fig. 5 Steady-state response for $\omega = 2, \delta = 0.5, \beta = 10, \gamma = 10, \mu = 1000, F_0 = 0.4$

Hence, to find the steady state response, the time-dependent terms in Equations (37) and (38) are set to zero, namely $a' = 0, \eta' = 0$. With this, Equations (37) and (38) become:

$$\frac{\delta a}{2} = -\frac{1}{\omega} \left[\frac{5}{16} Ra^4 \gamma + \frac{35}{64} \mu Ra^6 + \frac{35}{16} \mu R^3 a^4 \right] \sin \eta \tag{39}$$

$$\left[a\sigma - \frac{1}{\omega} \beta \left(\frac{3}{8} a^3 + 3R^2 a \right) - \frac{5}{\omega} \gamma \left(\frac{5}{16} a^5 + \frac{15}{2} R^2 a^3 + 15R^4 a \right) - \frac{5}{\omega} \mu \left(\frac{35}{128} a^7 + \frac{21}{16} R^2 a^5 + \frac{315}{4} R^4 a^3 + 70R^6 a \right) \right] = \frac{1}{\omega} \left[\frac{5}{16} Ra^4 \gamma + \frac{42}{64} \mu Ra^6 + \frac{35}{16} \mu R^3 a^4 \right] \cos \eta \tag{40}$$

Squaring Equations (39) and Eq. (40) and adding the resulting equations, the following expression is obtained for the detuning parameter σ :

$$\sigma = \frac{1}{\omega} \left[\beta \left(\frac{3}{8} a^2 + 3R^2 \right) + \gamma \left(\frac{5}{16} a^4 + \frac{15}{2} R^2 a^2 + 15R^4 \right) + \mu \left(\frac{35}{128} a^6 + \frac{21}{16} R^2 a^4 + \frac{315}{4} R^4 a^2 + 70R^6 \right) \right] \pm \sqrt{\left(\frac{5}{\omega} \right)^2 \left\{ \frac{15}{16} a^4 R \gamma + \frac{42}{64} Ra^6 \mu + \frac{35}{16} R^3 a^4 \mu \right\}^2 \left[1 - \left(\frac{\delta a}{2} \right)^2 \omega^2 \left(\frac{1}{\frac{5a^4 \gamma R}{16} + \frac{35a^6 R \mu}{64} + \frac{35a^4 R^3 \mu}{16}} \right)^2 \right]} \tag{41}$$

Now plugging $\sigma = \frac{1}{\varepsilon}(\Omega - \omega)$ into Eq. (41), the following equation for the frequency response is obtained:

$$\frac{\Omega}{\omega} = 5 + \frac{\varepsilon}{\omega} \left[A \pm \frac{5B}{2C} \sqrt{\left(\frac{4}{a^2 \omega^2} \right) B^2 - \delta^2} \right] \tag{42}$$

where

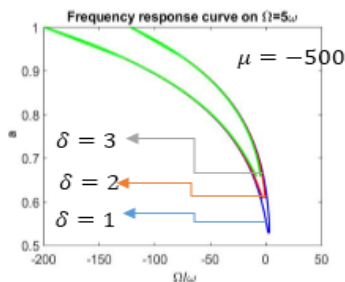
$$A = \frac{5}{\omega} \left\{ \beta \left(\frac{3}{8} a^2 + 3R^2 \right) + \gamma \left(\frac{5}{16} a^4 + \frac{15}{2} R^2 a^2 + 15R^4 \right) + \mu \left(\frac{35}{128} a^6 + \frac{21}{16} R^2 a^4 + \frac{315}{4} R^4 a^2 + 70R^6 \right) \right\}$$

$$B = \frac{15}{16} a^4 R \gamma + \frac{42}{64} Ra^6 \mu + \frac{35}{16} R^3 a^4 \mu, \quad C = \frac{5a^4 \gamma R}{16} + \frac{35a^6 R \mu}{64} + \frac{35a^4 R^3 \mu}{16}$$

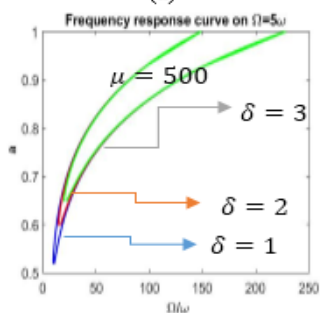
The amplitude response for subharmonic resonance is then given:

$$u(t) = a \cos\left(\frac{1}{5}\Omega t - \gamma\right) + \frac{F}{\omega^2 - \Omega^2} \cos(\Omega t) + O(\epsilon) \quad (43)$$

Variation in amplitude with frequency at the subharmonic resonance, that is, $\Omega = 5\omega$ under the effect of damping, force, and septic nonlinearity, is shown in Fig. 6 and 7. Fig. 6 depicts that the amplitude a bends to the right for the positive value of septic nonlinearity (Fig. 6a), while it bends to the left for the negative values of nonlinear parameter values (Fig. 6b). However, the amplitude a seems to converge to a line by increasing the damping parameter δ . Fig. 7 shows the relationship between the damping parameter δ , excitation term R and septic nonlinearity parameter μ . By increasing the damping, forcing, and septic nonlinearity parameter values, the amplitude converges to the specific branch value rather than multiple branch values.

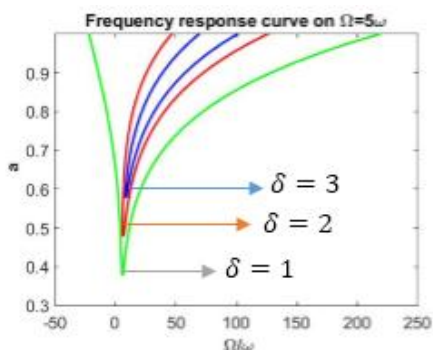


(a)

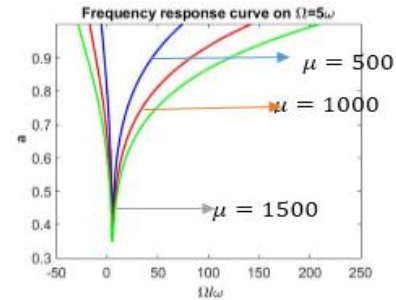


(b)

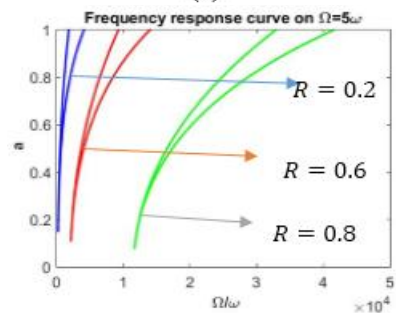
Fig. 6 Variation of amplitude with frequency under damping and nonlinearity for $\omega = 2$, $\beta = 10$, $\gamma = 10$, $R = 0.1$ (a) $\mu < 0$ (b) $\mu > 0$



(a)



(b)



(c)

Fig. 7 Variation of amplitude with frequency for $\omega = 2$ under the effect of (a) damping δ , (b) septic nonlinearity, and μ (c) forcing term R

2.3.2. Case-2: $\Omega = \frac{1}{5}\omega$ or $5\Omega = \omega$ (Super-Harmonic Resonance)

In this case, the nearness of the excitation frequency to the natural frequency is expressed by introducing the detuning parameter σ as

$$5\Omega = \omega + \epsilon\sigma \quad (44)$$

Substituting Eq. (44) into Eq. (27) and adopting a similar procedure as carried out in case I, the frequency response curve and amplitude response curve are obtained in Fig. 8.

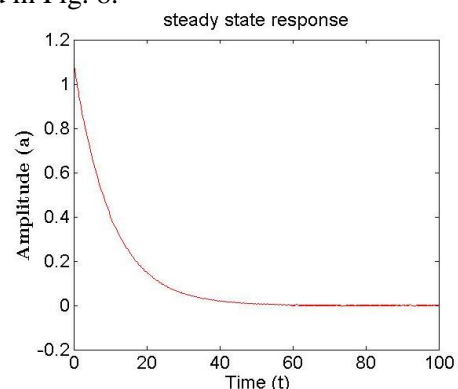


Fig. 8 Steady-state response for $\omega = 2$, $\delta = 0.5$, $\beta = 10$, $\gamma = 10$, $\mu = 1000$, $R = 0.4$

$$\begin{aligned} \frac{\Omega}{\omega} &= \frac{1}{5} + \frac{\epsilon}{\omega} \left[\beta \left(\frac{3}{8} a^2 + 3R^2 \right) + \gamma \left(\frac{5}{16} a^4 + \frac{15}{2} R^2 a^2 + 15R^4 \right) \right. \\ &+ \mu \left(\frac{35}{128} a^6 + \frac{105}{8} R^2 a^4 + \frac{315}{4} R^4 a^2 + 70R^6 \right) \\ &\left. \pm \frac{1}{2} \frac{\left(\gamma R^5 + 21R^5 \mu + \frac{21}{2} R^5 \mu a^2 + 7R^7 \mu \right)}{\left(\gamma R^5 - 21R^5 \mu + \frac{21}{2} R^5 \mu a^2 + 7R^7 \mu \right)} \sqrt{\frac{4}{a^2 \omega^2} \left\{ \frac{\gamma R^5 - 21R^5 \mu}{2} \right\}^2 - \delta^2} \right] \quad (45) \end{aligned}$$

The amplitude response u in the superharmonic resonance case is given as:

$$u(t) = a \cos(5\Omega t - \gamma) + \frac{F}{\omega^2 - \Omega^2} \cos(\Omega t) + O(\epsilon) \quad (46)$$

The steady-state response in terms of frequency response is shown in Fig. 9 and 10. These figures show the variation in amplitude with frequency at the super harmonic resonance, that is, $\Omega = \frac{1}{5}\omega$ under the effect of damping, force, and septic nonlinearity. Fig. 9 depicts that the sign of the septic nonlinearity parameter μ matters, that is, with a positive value of parameter μ , the amplitude a bends to the right, whereas with a negative value, it bends to the left.

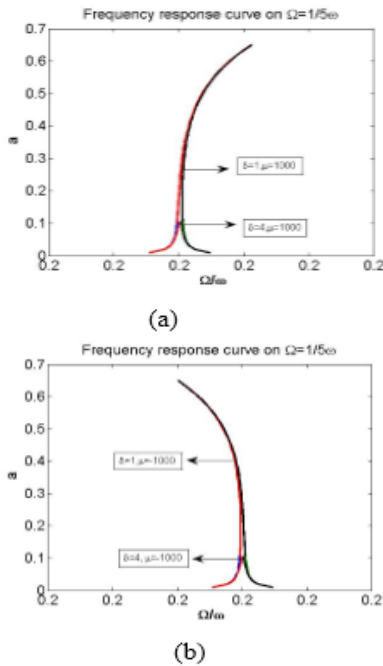


Fig. 9 Variation of amplitude with frequency for $\omega = 2$, $\beta = 10$, $\gamma = 10$, $R = 0.1$: (a) $\mu > 0$; (b) $\mu < 0$

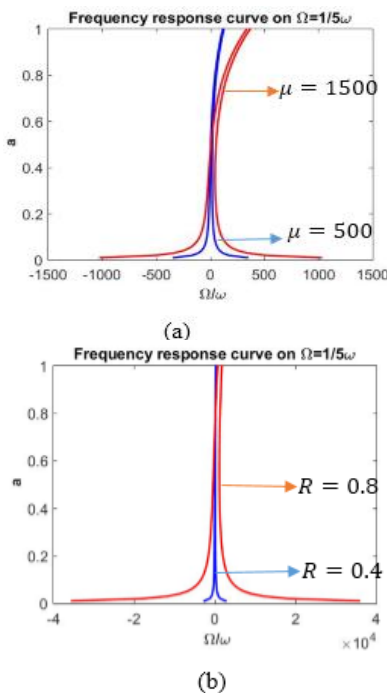


Fig. 10 Variation of amplitude with frequency for $\omega = 2$ with (a) septic nonlinearity μ and (b) forcing term R

However, the amplitude may converge to a specific value by increasing the damping. Fig. 10 shows the relationship between the excitation parameter R and the septic nonlinearity parameter μ versus the frequency ratio. Fig. 10a shows that the amplitude a shifts to the left with increasing positive value of nonlinear parameter μ . While Fig. 10b depicts that the domain of frequency ratio reduces as the excitation parameter R decreases.

2.3.3. Case-3: $\Omega \sim 7\omega$ (Subharmonic Resonance)

In this case, the nearness of the excitation frequency Ω with the natural frequency ω is expressed by the detuning parameter σ as:

$$\Omega = 7\omega + \epsilon\sigma \quad (47)$$

By following a similar procedure as discussed for Case-I and Case-II resonance cases, the following relation for the frequency response curve is obtained:

$$\frac{\Omega}{\omega} = 7 + \frac{\epsilon}{\omega} \left[\frac{7}{\omega} \left\{ \beta \left(\frac{3}{8}a^2 + 3R^2 \right) + \gamma \left(\frac{5}{16}a^4 + \frac{15}{2}R^2a^2 + 15R^4 \right) + \mu \left(\frac{35}{128}a^7 + \frac{105}{8}R^2a^5 + \frac{315}{4}R^4a^3 \right) \right\} \pm \frac{7}{2} \sqrt{\frac{49}{1024}\mu R^2a^{10} - \delta^2} \right] \quad (48)$$

Thus, the amplitude response u in this resonance case is given as Eq. (49) and Fig. 11:

$$u(t) = a \cos\left(\frac{1}{7}\Omega t - \gamma\right) + \frac{F}{\omega^2 - \Omega^2} \cos(\Omega t) + O(\epsilon) \quad (49)$$

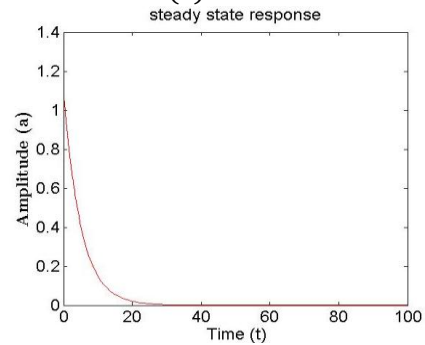
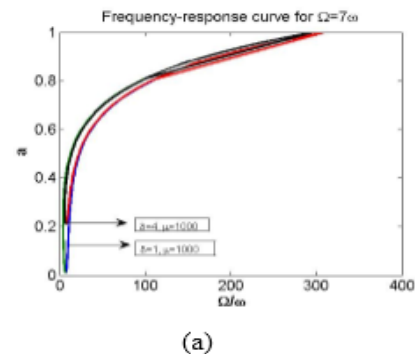


Fig. 11 Steady-state response for $\omega = 8$, $\delta = 0.5$, $\beta = 10$, $\gamma = 10$, $\mu = 100$, $R = 0.1$

Variation in amplitude with frequency at the subharmonic resonance, i.e., $\Omega = 7\omega$ under the effect of damping, force, and septic nonlinearity, is shown in Fig. 12 and 13.



(a)

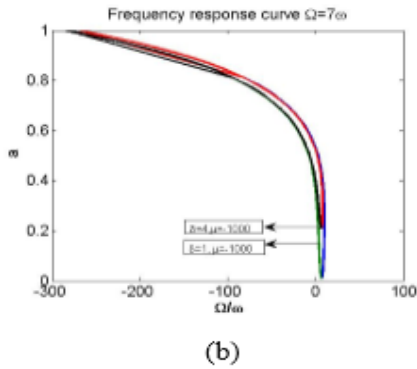


Fig. 12 Frequency response curve for $\omega = 2$, $\beta = 10$, $\gamma = 10$, $R = 0.1$ with (a) $\delta > 0$, $\mu > 0$ and (b) $\delta > 0$, $\mu < 0$

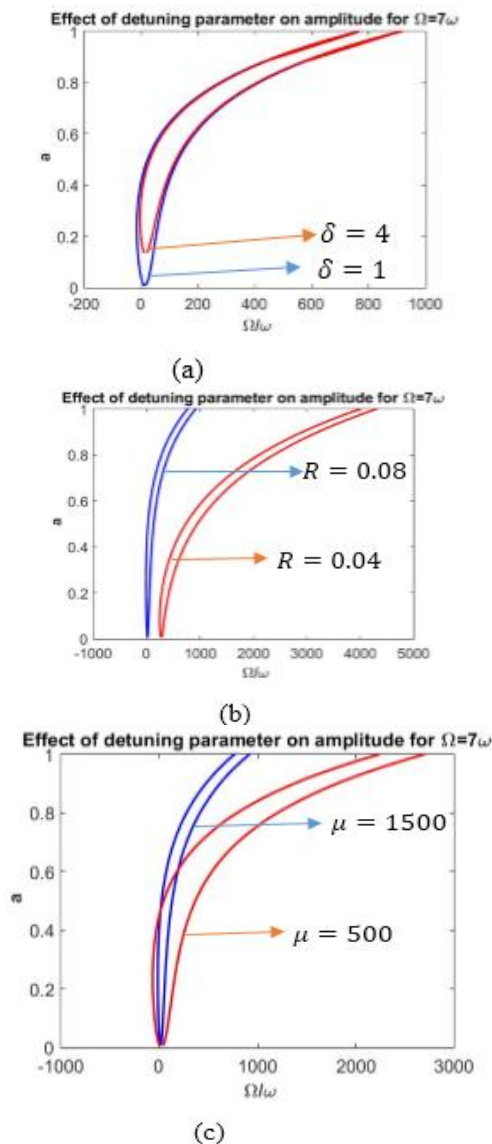


Fig. 13 Variation of amplitude with frequency for $\omega = 2$ under the effect of (a) damping δ , (b) forcing term R , and (c) septic nonlinearity μ

Fig. 12 depicts that the sign of septic nonlinearity matters, that is, with a positive value of the septic nonlinearity parameter, the nonlinear bends to the right and with a negative value, it bends to the left. However, the amplitude may converge to a specific value by increasing the damping. Fig. 13 shows the

relationship between damping, forcing, and septic nonlinearity parameters. By increasing the damping, forcing, and septic nonlinearity parameters, the amplitude converges to the specific branch value rather than multiple branch values, as occurs in nonlinear case.

2.3.4. Case-4: $\Omega \sim \frac{1}{7}\omega$ or $7\Omega = \omega$

In order to express the nearness of the excitation frequency Ω with the natural frequency ω of the system, the detuning parameter σ is introduced, which is of $O(1)$, so it follows:

$$7\Omega = \omega + \varepsilon\sigma \quad (50)$$

By following a similar procedure as discussed above, the following relation for the frequency response curve is obtained for the resonance case

$$\Omega \sim \frac{1}{7}\omega:$$

$$\frac{\Omega}{\omega} = 1 + \left[\left(\beta \left(\frac{3}{8}a^2 + 3R^2 \right) + \gamma \left(\frac{5}{16}a^4 + \frac{5}{12}a^2R^2 + 15R^4 \right) \right) + \mu \left(\frac{35}{128}a^6 + \frac{105}{8}R^2a^4 + \frac{315}{4}R^4a^2 \right) + 70R^6 \right] \pm \frac{1}{2} \sqrt{\frac{\mu^2 R^2}{\omega^2} - \delta^2} \quad (51)$$

The amplitude response u is then given as:

$$u(t) = a \cos(7\Omega t - \gamma) + \frac{F}{\omega^2 - \Omega^2} \cos(\Omega t) + O(\varepsilon) \quad (52)$$

The variation of amplitude a versus time t at the super harmonic resonance, that is, $\Omega = \frac{1}{7}\omega$ is shown in the Fig. 14. The fluctuation in amplitude with frequency under the effect of damping parameter δ , excitation parameter R and septic nonlinearity parameter μ is shown in Fig. 15 and 16. Under the effect of damping parameter and nonlinearity parameter μ , Fig. 15 depicts that the sign of septic nonlinearity parameter matters, that is, with the positive value of parameter μ , the amplitude a bends to the right whereas with negative value, it bends to the left.

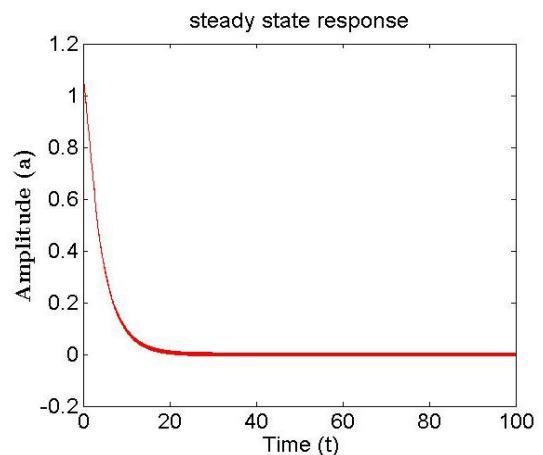


Fig. 14 Steady-state response for $\omega = 8$, $\delta = 0.5$, $\beta = 10$, $\gamma = 10$, $\mu = 100$, $R = 0.4$

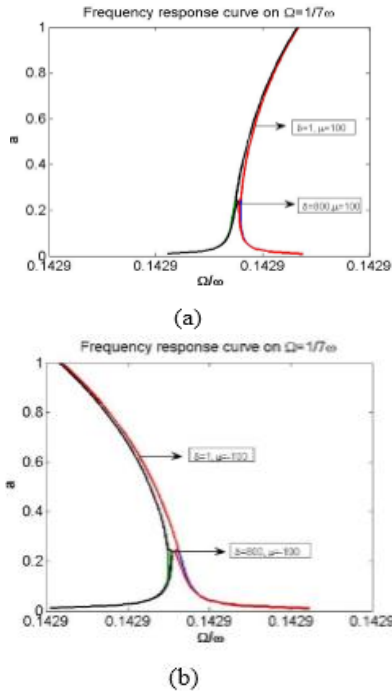


Fig. 15 Variation of amplitude with frequency for $\omega = 2$, $\beta = 10$, $\gamma = 10$, $R = 0.2$: (a) $\delta > 0$, $\mu > 0$ and (b) $\delta > 0$, $\mu < 0$

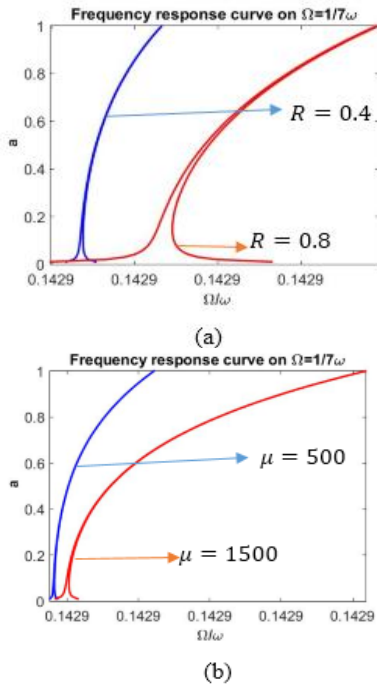


Fig. 16 Variation of amplitude with frequency for $\omega = 2$ under the effect of (a) forcing term R and (b) septic nonlinearity μ

However, the amplitude may converge to some specific value by increasing the damping. Fig. 16 shows the relationship between the forcing parameter and the R and septic nonlinearity parameter μ . By reducing the excitation parameter R and nonlinear parameter μ , it can be clearly seen in Fig. 16a and 16b that the amplitude a converges to the specific branch of values subject to the frequency ratio.

3. Conclusion

In this paper, the authors studied the nonlinear dynamics of a damped Duffing oscillator under the effect of external excitation. The authors considered both weak and strong external excitations in the oscillator system. The external excitation is considered to be harmonic time-varying excitation. Furthermore, the damping parameter and nonlinear parameters are considered constant and small, that is, of $O(\epsilon)$. Mathematically, the dynamics of the damped Duffing oscillator are expressed as second-order, seventh-degree nonhomogeneous nonlinear ordinary differential equations with constant coefficients. It is important to mention that the Duffing oscillator with damping and time-varying external excitation with seventh-order nonlinearity has not yet been studied. To construct the approximate analytical solution of the system, a two timescale perturbation method is used. In the case of weak external excitation, $F(t) = O(\epsilon)$, it turned out that the resonances occur only when the excitation frequency Ω is near or equal to the natural frequency ω of the system, that is, when $\Omega = \omega$, which is known as a primary resonance. The frequency response of the Duffing oscillator system is computed at the primary resonance. It is found that the amplitude reduces to zero as the time increases, that is, only the steady-state solution is possible for a weakly excited system. In the steady-state case, the variation of the amplitude with a frequency ratio under the effect of damping, excitation, and nonlinear parameters is obtained. It is found that the amplitude bends to the right for positive values of the septic nonlinearity parameter and to the left for negative values of the nonlinear parameter. In case of strong external excitation, that is $F(t) = O(1)$, it is found out that the resonances occur if the excitation frequency Ω is near or equal to one time, three times, one-third times, five times, one-fifth times, seven times and one-seventh times of the natural frequency ω of the system, that is, when $\Omega = \omega, 3\omega, \frac{1}{3}\omega, 5\omega, \frac{1}{5}\omega, 7\omega, \frac{1}{7}\omega$. Both resonant and the non-resonant cases are considered for strongly excited systems. The unsteady state solution for the non-resonant region in terms of amplitude response is computed. It turned out that the response of the system behaves like a linear system as the time increases, that is, remains constant as the time progresses. In the resonant cases, only four resonant cases are taken into account: $\Omega = 5\omega, \frac{1}{5}\omega, 7\omega, \frac{1}{7}\omega$. It is obtained that the amplitude response reduces to zero as the time increases, that is, the steady-state solution is seen to turn up. The amplitude bends and shifts under the effects of septic nonlinear and excitation parameters, respectively.

References

[1] PAKDEMIRLI M., KARAHAN M. M. F., and BOYACI

- H. Forced Vibrations of strongly Nonlinear systems with multiple scales Lindstedt-Poincare Method. *Mathematical and Computational Applications*, 2011, 16(4): 879-889. <https://doi.org/10.3390/mca16040879>
- [2] RAMOS J. I. On Lindstedt-Poincare Techniques for the Quantic Duffing Equation. *Applied Mathematics and Computation*, 2007, 193(2): 303-310. <https://doi.org/10.1016/j.amc.2007.03.050>
- [3] PAKDEMIRLI M. Precession of a planet with the multiple scales Lindstedt-Poincare technique. *Zeitschrift fur Naturforschung*, 2015, 70(10): 829-834. <https://doi.org/10.1515/zna-2015-0312>
- [4] PAKDEMIRLI M., and SARI G. Solution of quadratic nonlinear problems with multiple scales Lindstedt Poincare method. *Mathematical and Computational Applications*, 2015, 20(2): 137-150. <https://doi.org/10.3390/mca20010150>
- [5] PAKDEMIRLI M., and SARI G. Perturbation solutions of the quantic Duffing equation with strong nonlinearities. *Communication in Numerical Analysis*, 2015, 1: 82-89. <http://dx.doi.org/10.5899/2015/cna-00230>
- [6] DAL F. Multiple time scales solution of an equation with quadratic and cubic nonlinearities having fractional-order derivative. *Mathematical and Computational Applications*, 2011, 16(1): 301-308. <https://doi.org/10.3390/mca16010301>
- [7] RAZZAK M. A., ALAM M. Z., and SHARIF M. N. Modified multiple time scale method for solving strongly nonlinear damped force vibration systems. *Results in Physics*, 2018, 8: 231-238. <https://doi.org/10.1016/j.rinp.2017.12.015>
- [8] KOVACIC I. The method of multiple scales for forced oscillators with some real-power nonlinearities in the stiffness and damping force. *Chaos, Solitons and Fractals*, 2011, 44(10): 891-901. <https://doi.org/10.1016/j.chaos.2011.07.006>
- [9] DEHRAJ S., SANDILO S. H., and MALOOKANI R. A. On applicability of truncation method for damped axially moving string. *Journal of Vibroengineering*, 2020, 22(2): 337-352. <https://doi.org/10.21595/jve.2020.21192>
- [10] DEHRAJ S., MALOOKANI R. A., and SANDILO S. H. On Laplace transform and (in) stability of externally damped axially moving string. *Journal of Mechanics of Continua and Mathematical Sciences*, 2020, 15(8): 282-298. <http://dx.doi.org/10.26782/jmcmcs.2020.08.00027>
- [11] DEHRAJ S., MALOOKANI R. A., and SANDILO S. H. On effects of viscous damping of harmonically varying axially moving string. *International Journal of Advanced and Applied Sciences*, 2020, 7(7): 48-55. <https://doi.org/10.21833/ijaas.2020.07.006>
- [12] AASOORI S. K., MALOOKANI R. A., SANDILO S. H., DEHRAJ S., and SHEIKH A. H. On transversal vibrations of an axially moving string under structural damping. *Journal of Mechanics of Continua and Mathematical Sciences*, 2020, 15 (8): 93-108. <https://www.journalimcmcs.org/journal/on-transversal-vibrations-of-an-axially-moving-string-under-structural-damping/>
- [13] MALIK K. H., DEHRAJ S., JAMALI S., SANDILO S. H., and AWAN, A. On the transversal vibrations of an axially moving beam under the influence of viscous damping. *Journal of Mechanics of Continua and Mathematical Sciences*, 2020, 15(10): 12-22. <https://www.journalimcmcs.org/journal/on-transversal-vibrations-of-an-axially-moving-beam-under-influence-of-viscous-damping/>
- [14] DEHRAJ S., MALOOKANI R. A., MEMON M., KHATRI A. R., MAITLO A. A., and NIZAMANI Z. On the Stability of the van der Pol-Mathieu-Duffing Oscillator under the Effect of Fast Harmonic Excitation. *Journal of Hunan University Natural Sciences*, 2022, 49(12): 265-273. <https://doi.org/10.55463/issn.1674-2974.49.12.27>
- [15] SEDIGH H. M., SHIRAZI K. H., and ATTARZADEH M. A. A study on the quantic nonlinear beam vibrations using asymptotic approximate approaches. *Acta Astronautica*, 2013, 91: 245-250. <https://doi.org/10.1016/j.actaastro.2013.06.018>
- [16] RAZZAK M. A., & MOLLA M. H. U. A new analytical technique for strongly nonlinear damped forced systems. *Ain Shams Engineering Journal*, 2015, 6(4): 1225-1232. <https://doi.org/10.1016/j.asej.2015.05.004>
- [17] KHAN Y., & WU Q. Homotopy perturbation transform method for nonlinear equations using He's polynomials. *Computers & Mathematics with Applications*, 2011, 61(8): 1963-1967. <https://doi.org/10.1016/j.camwa.2010.08.022>
- [18] HE J. H. Preliminary report on the energy balance for nonlinear oscillators. *Mechanics Research Communications*, 2002, 29(2-3): 107-111. [https://doi.org/10.1016/S0093-6413\(02\)00237-9](https://doi.org/10.1016/S0093-6413(02)00237-9)
- [19] EI-NAGGAR M. A., & ISMAIL G. M. Periodic solutions of the Duffing harmonic oscillator by He's energy balance method. *Journal of Applied and Computational Mechanics*, 2016, 2(1): 35-41. [10.22055/JACM.2016.12269](https://doi.org/10.22055/JACM.2016.12269)
- [20] NOURAZAR S., & MIRZABEIGY A. Approximate solution for nonlinear Duffing oscillator with damping effect using the modified differential transform method. *Scientia Iranica*, 2013, 20(2): 364-368. <https://doi.org/10.1016/j.scient.2013.02.023>
- [21] YANG Q. W., CHEN Y. M., LIU J. K., and ZHAO W. A modified variational iteration method for nonlinear oscillators. *International Journal of Nonlinear Sciences and Numerical Simulation*, 2013, 14(7-8): 453-462. <https://doi.org/10.1515/ijnsns-2011-045>
- [22] HUANG Y. J., & LIU H. K. A new modification of the variational iteration method for van der Pol equations. *Applied Mathematical Modelling*, 2013, 37(16-17): 8118-8130. <https://doi.org/10.1016/j.apm.2013.03.033>
- [23] VAHIDI A. R., AZIMZADEH Z., and MOHAMMADIFAR S. Restarted Adomian decomposition method for solving Duffing-van der pol equation. *Applied Mathematical Sciences*, 2012, 6(11): 499-507. <http://www.m-hikari.com/ams/ams-2012/ams-9-12-2012/vahidiAMS9-12-2012-3.pdf>
- [24] BISSANGA G. Application of the Adomian Decomposition Method to Solve the Duffing Equation and Comparison with the Perturbation Method. *Contemporary Problems in Mathematical Physics*, 2006: 372-377. https://doi.org/10.1142/9789812773241_002
- [25] ALY E. H., EBALD A., and RACH R. Advances in the Adomian decomposition method for solving two-point nonlinear boundary value problems with Neumann boundary conditions. *Computers & Mathematics with Applications*, 2012, 63(6): 1056-1065. <https://doi.org/10.1016/j.camwa.2011.12.010>
- [26] RACH R., WAZWAZ A. M., and DUAN J. S. A reliable modification of the Adomian decomposition method for higher-order nonlinear differential equations. *Kybernetes*, 2013, 42(2): 282-308.

<https://doi.org/10.1108/03684921311310611>

- [27] DEHRAJ S., MAITLO A. A., SIYAL W. A., MEMON M., ARAIN L. N., ARAIN L., and UMRANI K. A Comparison of the Adomian Decomposition Method and Variational Iteration Method for a Two-Dimensional Nonlinear Wave Equation. *Journal of Hunan University Natural Sciences*, 2023, 50(2): 28-37. <https://doi.org/10.55463/issn.1674-2974.50.2.3>
- [28] DEHRAJ S., MALOOKANI R. A., ARAIN M. B., and NIZAMANI N. Oscillating Flows of Fractionalized Second Grade Fluid with Slip Effects. *Punjab University Journal of Mathematics*, 2020, 51(11): 63-75. http://pu.edu.pk/images/journal/math/PDF/Paper-6_51_11_2019.pdf
- [29] DEHRAJ S., MALOOKANI R. A., AASOORI S. K., BHUTTO G. M., and ARAIN L. Exact solutions for fractionalized second grade fluid flows with boundary slip effects. *International Journal of Applied Mechanics and Engineering*, 2021, 26(1): 88-103. https://ui.adsabs.harvard.edu/link_gateway/2021IJAME..26a..88D/doi:10.2478/ijame-2021-0006
- [30] CHOWDHURY M. S. H., ALAL HOSEN M., AHMAD K., ALI M. Y., and ISMAIL A.F. Higher-order approximate solutions of strongly nonlinear cubic-quantum Duffing oscillator based on the harmonic balance method. *Results in Physics*, 2017, 7: 3962-3967. <http://dx.doi.org/10.1016/j.rinp.2017.10.008>

参考文献:

- [1] PAKDEMIRLI M., KARAHAN M. M. F., 和 BOYACI H. 多尺度林斯特-庞加莱方法的强非线性系统的受迫振动。 *数学和计算应用*, 2011, 16(4): 879-889. <https://doi.org/10.3390/mca16040879>
- [2] RAMOS J. I. 关于量子达芬方程的林斯特-庞加莱技术。 *应用数学与计算*, 2007, 193(2): 303-310. <https://doi.org/10.1016/j.amc.2007.03.050>
- [3] PAKDEMIRLI M. 使用多尺度林斯特-庞加莱技术进行行星进动。 *自然研究杂志*, 2015, 70(10): 829-834. <https://doi.org/10.1515/zna-2015-0312>
- [4] PAKDEMIRLI M., 和 SARI G. 用多尺度林斯特-庞加莱方法求解二次非线性问题。 *数学和计算应用*, 2015, 20(2): 137-150. <https://doi.org/10.3390/mca20010150>
- [5] PAKDEMIRLI M., 和 SARI G. 具有强非线性的量子达芬方程的扰动解。 *数值分析交流*, 2015, 1: 82-89. <http://dx.doi.org/10.5899/2015/cna-00230>
- [6] DAL F. 具有分数阶导数的二次和三次非线性方程的多时间尺度解。 *数学和计算应用*, 2011, 16(1): 301-308. <https://doi.org/10.3390/mca16010301>
- [7] RAZZAK M. A., ALAM M. Z., 和 SHARIF M. N. 改进的多时间尺度方法求解强非线性阻尼力振动系统。 *物理学成绩*, 2018, 8: 231-238. <https://doi.org/10.1016/j.rinp.2017.12.015>
- [8] KOVACIC I. 刚度和阻尼力具有一定实功率非线性的受迫振荡器的多尺度方法。 *混沌、孤子和分形*, 2011, 44(10): 891-901. <https://doi.org/10.1016/j.chaos.2011.07.006>
- [9] DEHRAJ S., SANDILO S. H., 和 MALOOKANI R. A. 阻尼轴向动弦截断法的适用性研究 *振动工程学报*, 2020, 22(2): 337-352. <https://doi.org/10.21595/jve.2020.21192>
- [10] DEHRAJ S., MALOOKANI R. A., 和 SANDILO S. H. 关于拉普拉斯变换和外部阻尼轴向移动弦的(内)稳定性。 *连续体力学与数学科学杂志*, 2020, 15(8): 282-298. <http://dx.doi.org/10.26782/jmcs.2020.08.00027>
- [11] DEHRAJ S., MALOOKANI R. A., 和 SANDILO S. H. 关于谐波变化的轴向运动弦的粘性阻尼的影响。 *国际先进与应用科学杂志*, 2020, 7(7): 48-55. <https://doi.org/10.21833/ijaas.2020.07.006>
- [12] AASOORI S. K., MALOOKANI R. A., SANDILO S. H., DEHRAJ S., 和 SHEIKH A. H. 关于结构阻尼下轴向移动弦的横向振动。 *连续体力学与数学科学杂志*, 2020, 15(8): 93-108. <https://www.journalimcms.org/journal/on-transversal-vibrations-of-an-axially-moving-string-under-structural-damping/>
- [13] MALIK K. H., DEHRAJ S., JAMALI S., SANDILO S. H., 和 AWAN, A. 粘性阻尼影响下轴向移动梁的横向振动。 *连续体力学与数学科学杂志*, 2020, 15(10): 12-22. <https://www.journalimcms.org/journal/on-transversal-vibrations-of-an-axially-moving-beam-under-influence-of-viscous-damping/>
- [14] DEHRAJ S., MALOOKANI R. A., MEMON M., KHATRI A. R., MAITLO A. A., 和 NIZAMANI Z. 快速谐波激励作用下范德波尔-马蒂厄-杜芬振荡器的稳定性。 *湖南大学自然科学学报*, 2022, 49(12): 265-273. <https://doi.org/10.55463/issn.1674-2974.49.12.27>
- [15] SEDIGH H. M., SHIRAZI K. H., 和 ATTARZADEH M. A. 使用渐近近似方法研究量子非线性梁振动。 *宇航学报*, 2013, 91: 245-250. <https://doi.org/10.1016/j.actaastro.2013.06.018>
- [16] RAZZAK M. A., 和 MOLLA M. H. U. 强非线性阻尼受力系统的新分析技术。 *艾因·沙姆斯工程杂志*, 2015, 6(4): 1225-1232. <https://doi.org/10.1016/j.asej.2015.05.004>
- [17] KHAN Y., 和 WU Q. 使用他多项式的非线性方程同伦摄动变换方法。 *计算机与数学及其应用*, 2011, 61(8): 1963-1967. <https://doi.org/10.1016/j.camwa.2010.08.022>
- [18] HE J. H. 关于非线性振荡器能量平衡的初步报告。 *力学研究通讯*, 2002, 29(2-3): 107-111. [https://doi.org/10.1016/S0093-6413\(02\)00237-9](https://doi.org/10.1016/S0093-6413(02)00237-9)
- [19] EI-NAGGAR M. A., 和 ISMAIL G. M. 贺氏能量平衡法求解达芬谐振子的周期解。 *应用与计算力学杂志*, 2016, 2(1): 35-41. [10.22055/JACM.2016.12269](https://doi.org/10.22055/JACM.2016.12269)
- [20] NOURAZAR S., 和 MIRZABEIGY A. 具有阻尼效应的非线性达芬振子的修正微分变换方法的近似解。 *伊朗科学协会*, 2013, 20(2): 364-368. <https://doi.org/10.1016/j.scient.2013.02.023>
- [21] YANG Q. W., CHEN Y. M., LIU J. K., 和 ZHAO W. 非线性振子的改进变分迭代方法。 *国际非线性科学与数值模拟杂志*, 2013, 14(7-8): 453-462. <https://doi.org/10.1515/ijnsns-2011-045>
- [22] HUANG Y. J., 和 LIU H. K. 范德波尔方程变分迭代法的新修改。 *应用数学建模*, 2013, 37(16-17): 8118-8130. <https://doi.org/10.1016/j.apm.2013.03.033>
- [23] VAHIDI A. R., AZIMZADEH Z., 和 MOHAMMADIFAR S. 重新启动了亚多米安分解方法来

求解杜芬-范德波尔方程。应用数学科学, 2012, 6(11): 499-507. <http://www.m-hikari.com/ams/ams-2012/ams-9-12-2012/vahidiAMS9-12-2012-3.pdf>

[24] BISSANGA G. 应用亚多米安分解法求解达芬方程并与摄动法比较。数学物理的当代问题, 2006: 372-377. https://doi.org/10.1142/9789812773241_002

[25] ALY E. H., EBAID A., 和 RACH R. 求解具有诺伊曼边界条件的两点非线性边值问题的亚多米安分解方法的进展。计算机与数学及其应用, 2012, 63(6): 1056-1065. <https://doi.org/10.1016/j.camwa.2011.12.010>

[26] RACH R., WAZWAZ A. M., 和 DUAN J. S. 高阶非线性微分方程亚多米安分解方法的可靠修正。控制网络, 2013, 42(2): 282-308. <https://doi.org/10.1108/03684921311310611>

[27] DEHRAJ S., MAITLO A. A., SIYAL W. A., MEMON M., ARAIN L. N., ARAIN L., 和 UMRANI K. 二维非线性波动方程的亚多米安分解法与变分迭代法的比较。湖南大学自然科学学报, 2023, 50(2): 28-37. <https://doi.org/10.55463/issn.1674-2974.50.2.3>

[28] DEHRAJ, S., MALOOKANI, R. A., ARAIN, M. B., 和 NIZAMANI, N. 具有滑移效应的分级二级流体的振荡流。旁遮普大学数学杂志, 2020, 51(11): 63-75. http://pu.edu.pk/images/journal/math/PDF/Paper-6_51_11_2019.pdf

[29] DEHRAJ S., MALOOKANI R. A., AASOORI S. K., BHUTTO G. M., 和 ARAIN L. 具有边界滑移效应的分段二级流体流动的精确解。国际应用力学与工程杂志, 2021, 26(1): 88-103. https://ui.adsabs.harvard.edu/link_gateway/2021IJAME..26a..88D/doi:10.2478/ijame-2021-0006

[30] CHOWDHURY M. S. H., ALAL HOSEN M., AHMAD K., ALI, M. Y., 和 ISMAIL A.F. 基于谐波平衡法的强非线性三次量子达芬振子的高阶近似解。物理学成绩, 2017, 7: 3962-3967. <http://dx.doi.org/10.1016/j.rinp.2017.10.008>